Princeton's Net-Zero America study
Annex L: Hydrogen and Synthetic Fuels/Feedstocks Transition

Eric D. Larson, Senior Research Engineer
Andlinger Center for Energy and the Environment, Princeton University

With contributions from Robert H. Williams (Senior Research Scientist Emeritus, Andlinger Center, Princeton), Andrew Pascale (Postdoctoral Research Associate, Andlinger Center, Princeton; Senior Research Fellow, Dow Centre for Sustainable Engineering Innovation, The University of Queensland), Paris L. Blaisdell-Pijuan (PhD candidate, Electrical and Computer Engineering, Princeton), Fangwei Cheng (Postdoctoral Research Associate, Andlinger Center, Princeton), and Claire Wayner (Undergraduate class of 2022, Princeton).

1 August 2021

Contents

1. Introduction 2
1.1. Clean fuels and feedstocks 2
1.2. Context and perspective 2
2. Hydrogen and synthetic fuels in net-zero emissions pathways 3
2.1. Aggregated national results 3
2.2. Coarse geographic distribution of hydrogen producers and users 8
2.3. Notional downscaled siting of hydrogen producers and users 10
2.4. Regional hydrogen pipeline system vignettes 11
Appendix A: Technology Performance and Cost Assumptions 15
Appendix B: Visualization of Hypothetical Regional H_2 pipelines 19
References 20

1. Introduction

1.1. Clean fuels and feedstocks

About half of all final energy services are delivered by electricity in our suite of high end-use electrification net-zero emissions pathways (E+, E+RE-, E+RE+), leaving a significant amount of services that must be provided by fuels, including in difficult-to-electrify uses, such as aviation and high-temperature heat and chemical feedstocks. The less-high electrification pathways (E- and E-B+) require still more fuels due to less electrification of vehicles and buildings. The RIO model has three options for supplying net carbon-free fuels:

1) petroleum-derived fuels combined with negative emissions to offset their combustion emissions. (Negative emissions can be achieved using bioenergy conversion with CO_2 capture and storage (BECCS) or by direct air capture (DAC) and storage of CO_2);
2) hydrogen produced from natural gas with CO_2 capture and storage, from biomass with or without CO_2 capture, or by electrolysis of water using solar, wind, or other carbon-free electricity; and
3) liquid or gaseous hydrocarbon fuels either synthesized from hydrogen and captured CO_2 or made from biomass with or without capture of byproduct CO_2.

The body of this annex describes the fuels transitions embodied in our five net-zero emissions energy-system pathways described in the main report. The transition has been modeled for 14 geographic regions representing the continental U.S. Some notional conceptualizations of fuels production and use at finer geographic resolutions are also presented here. Finer resolution downscaling analysis is ongoing at Princeton.

The appendix to this annex gives performance and cost assumptions for biomass conversion, hydrogen, and synthetic fuels production technologies included in our modeled net-zero emissions pathways, along with hydrogen delivery and storage assumptions. Additionally, Annex J [1] discusses assumed hydrogen use in iron and steel production through the transition.

1.2. Context and perspective

Among clean fuels in the modeled net-zero pathways, only hydrogen is produced and used in significant quantities today in the U.S.: about 11 million metric tonnes per year, with predominant uses being in petroleum refining (57%) and ammonia and methanol production (38%) [2]. Hydrogen production today is accordingly located at or near these industrial demands (Figure 1). The dominant technology for production of hydrogen today is steam methane reforming (SMR). When hydrogen is not being produced where it is used, trucks or pipelines bring it to users. About 1,600 miles of hydrogen pipelines serve customers today, primarily along the Gulf Coast in the Louisiana and Texas region, with smaller capacity lines in Illinois near Indiana along Lake Michigan, and in the metropolitan Los Angeles area.

In all Net-Zero America pathways, hydrogen use broadens across the economy by 2050 into a wide variety of intermediate and consumer uses, growing by a factor of five in the E+ and E+RE- pathways and by greater amounts in the other pathways, including by a factor of 12 for the E+RE+ pathway. (A recent hydrogen road map for the U.S. [2] projects a 6- to 7-fold increase in hydrogen use by 2050.) For perspective, total hydrogen production in 2050 in the E+

scenario (59 million tonnes, or 8.3 EJ on a higher heating value (HHV) basis, EJ_{HHV}*) is equivalent to current total natural gas use in the U.S. (~35 EJ_{HHV}, or 31 trillion standard cubic feet, per year [3]) on a volumetric basis at 100 bar pressure, the upper end of the range of pressures typical for interstate natural gas transmission pipelines [4] and existing hydrogen pipelines serving industrial customers [5]. Global hydrogen production today is about 115 million tonnes/year (2018 estimate) [6].

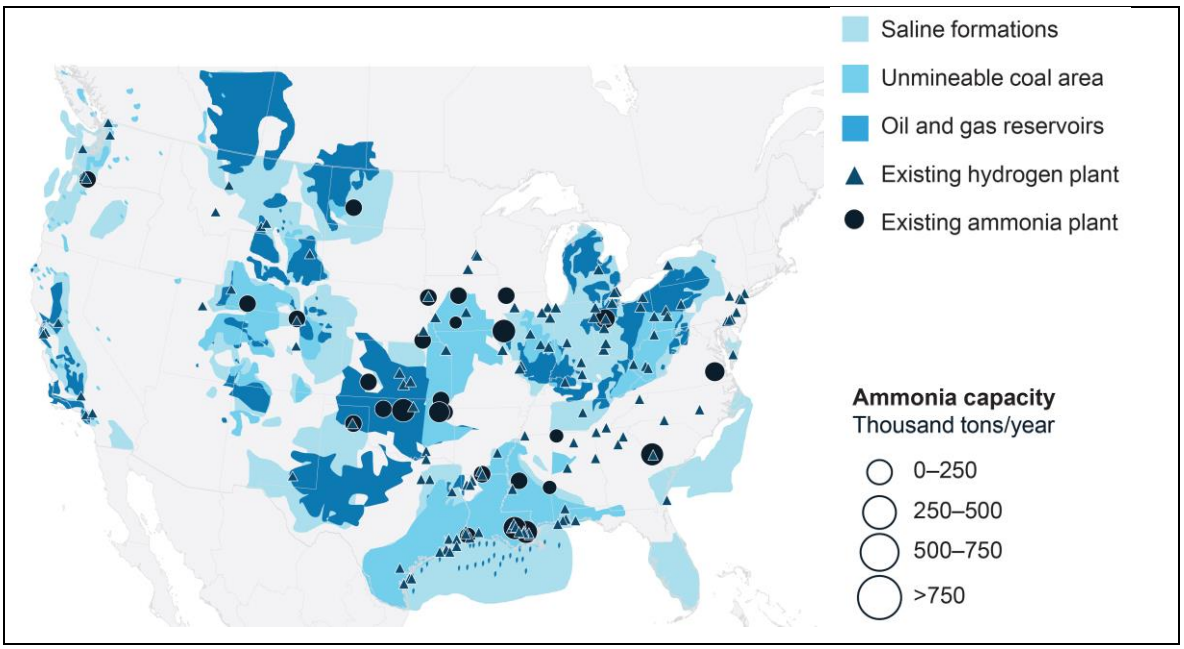

Figure 1. Hydrogen production facilities in the U.S. today. Also shown are existing ammonia plants, which are major consumers of hydrogen. Also indicated are areas where the subsurface is judged suitable for storage of CO_2, such as CO_2 captured in the process of making hydrogen from natural gas. Source [2].

2. Hydrogen and synthetic fuels in net-zero emissions pathways

2.1. Aggregated national results

Figure 2 through Figure 6 show nationally aggregated hydrogen production and use across each of the five modeled net-zero pathways.

Hydrogen production in the E+ pathway is shown in Figure 2 (left panel). SMR production begins falling in the late 2020s and is fully replaced by other sources by 2050. By 2030 autothermal reforming with CO_2 capture (ATR-CC), which is estimated to be a lower-cost option than SMR with CO_2 capture at commercial scale [7], accounts for about 1/3 of supply nationally. ATR-CC production continues to grow through 2045 before dropping in the final modeling period. Meanwhile, biomass conversion to hydrogen with CO_2 capture expands rapidly from 2030, accounting for 50% of all hydrogen production in 2035, 70% in 2045, and 60% in 2050. Electrolysis for hydrogen production first becomes competitive and then grows rapidly during the final decade of the transition, contributing 1/3 of total supply by 2050.

* The energy contents of fuels in the Net Zero America report and annexes are reported as higher heating values, unless otherwise noted. Appendix Table 1 gives higher and lower heating values for key fuels.

Hydrogen use in the E+ pathway is shown in Figure 2, right panel. Bulk chemicals demand grows slowly and continues to be an important hydrogen user through the transition. Additional industrial uses (steam generation, reduction of iron, and others) grow starting in the 2030s. By 2050 direct industrial use of hydrogen accounts for about 1/3 of total demand. The use of hydrogen in fuel cell trucks begins growing in the 2030s and by 2050 accounts for about 20% of total demand. The use of hydrogen as an input, along with CO_2, to the synthesis of Fischer-Tropsch liquid fuels [in the reverse-water-gas-shift-Fischer-Tropsch Synthesis (RWGS-FTS) technology described in Appendix Table 2] grows rapidly in the 2040s and accounts for 1/3 of total hydrogen demand by 2050. About 7% of hydrogen demand in 2050 is at power plants, where it augments pipeline gas to power combustion turbines or gas turbine combined cycles in mixtures up to 60/40 hydrogen/natural gas (HHV energy basis). Finally, a small amount of hydrogen is injected in 2050 into the natural gas pipeline system to create "hythane" (up to 7% H_2 on a HHV energy basis).

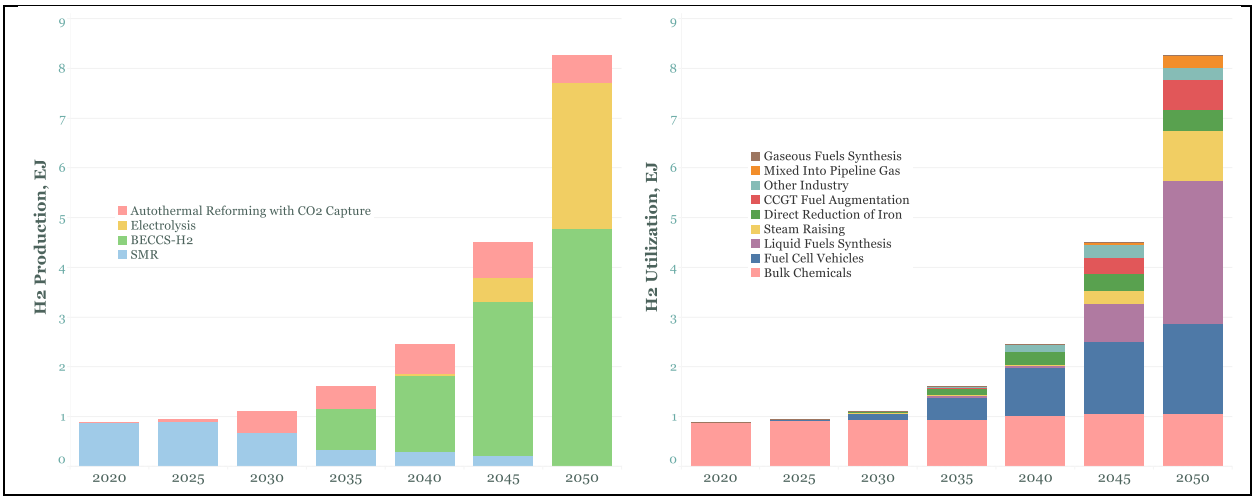

Figure 2. Production and use of H_2 (higher heating value energy content) to 2050 in the E+ scenario.

The distribution of hydrogen sources in the E- pathway (Figure 3, left panel) shows biomass playing an important role, as in the E+ pathway. However, unlike in E+, SMR production ceases by 2035, and there are smaller contributions from ATR-CC through the transition. Electrolysis grows instead. These shifts in the production mix from E+ to E- are explained by the fact that additional fossil fuels are used to meet vehicle and space heating demands in E-. The resulting emissions are difficult to capture due to their distributed nature, and so the modeling chooses other places in the energy system where emissions can be reduced, including from SMR and ATR-CC. With ATR-CC a portion of the produced CO_2 is not captured (Appendix Table 3).

As for hydrogen uses in E- (Figure 3, right panel), transportation uses are smaller than in E+ because the assumed penetration of fuel cell electric vehicles over time is lower (similar to the slower penetration rate for battery electric vehicles), and liquid fuels synthesis plays an earlier and much more significant role in the transition. Hydrogen also replaces more pipeline gas in industrial steam generation earlier in the transition relative to E+. This helps compensate for greater emissions from vehicles and space heating in E-.

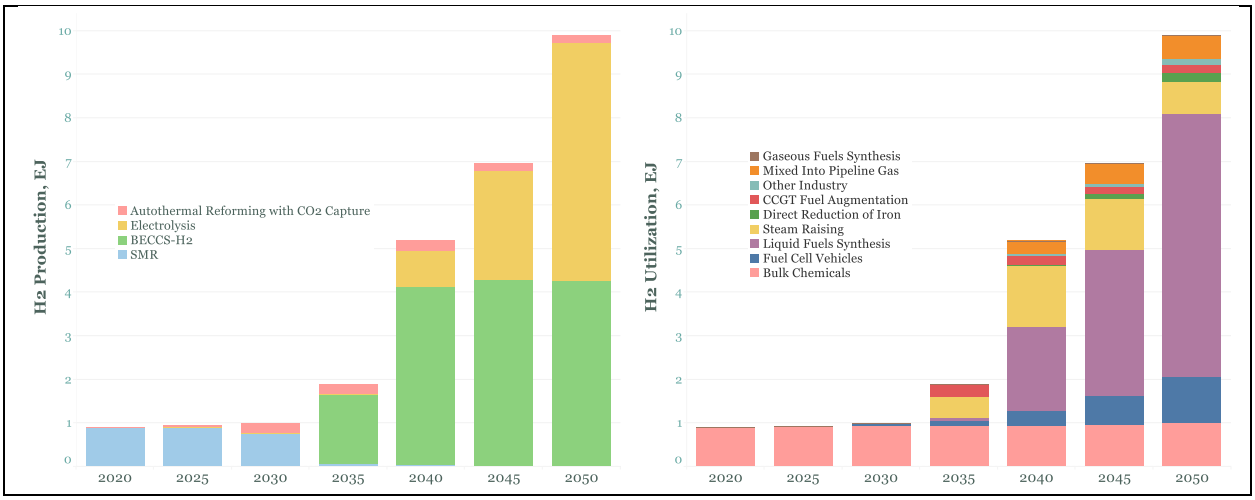

Figure 3. Production and use of H_2 (higher heating value energy content) to 2050 in the E- scenario.

The timing and distribution by technology of hydrogen production and use in the E- B+ pathway (Figure 4) is similar to those in E-, except that biomass-derived hydrogen plays a larger role due to the greater availability of biomass in that pathway. Correspondingly, electrolysis plays a smaller role.

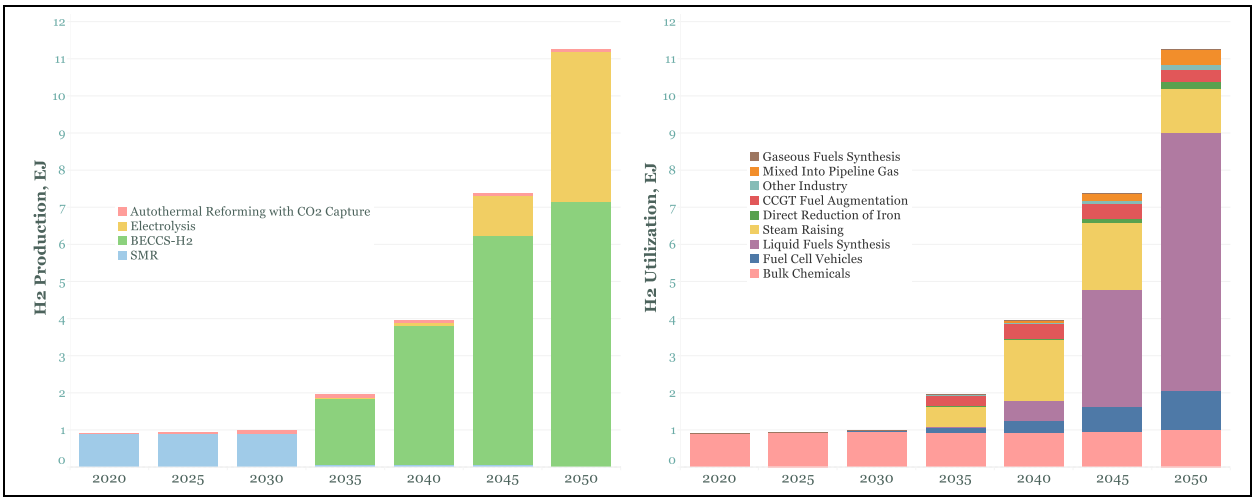

Figure 4. Production and use of H_2 (higher heating value energy content) to 2050 in the E- B+ scenario.

Hydrogen in E+ RE- (Figure 5) shows significant departures from the other three pathways. Biomass continues to be an important hydrogen provider, but most of the rest of the hydrogen is supplied by ATR-CC. The latter replaces electrolytic production, whose role is reduced due to the reduced deployment of solar and wind generation. On the demand side, the dominant H_2 use after 2030 is in substitution for natural gas in industrial steam generation, in gas turbine power generation, and in the pipeline gas system itself. Liquid fuels synthesis plays a minor role.

In the E+ RE+ pathway (Figure 6), total hydrogen production and use is much higher than in any of the other four pathways, because there is greater demand by 2050 for synthetic liquid fuels due to the exogenously-imposed constraint of no fossil fuel use in 2050. Production of hydrogen via SMR grows through 2040 before declining to zero by 2050. Electrolytic production matches SMR production in 2040 and grows very rapidly after that. BECCS-H_2

plays a lesser role, because biomass is used primarily instead to make pyrolytic oil as a substitute for petrochemical feedstocks that would otherwise have been provided by fossil fuels.

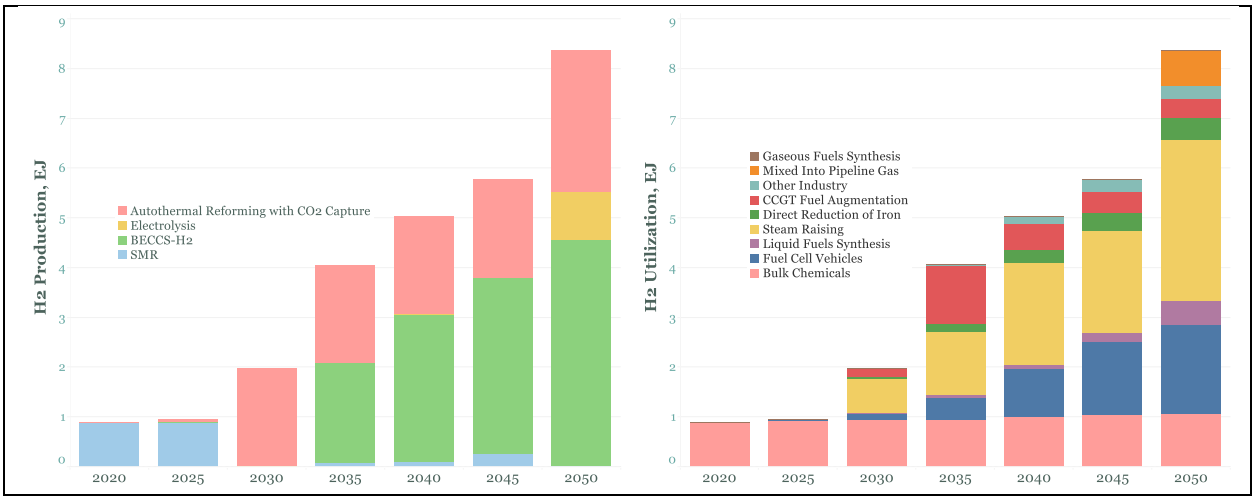

Figure 5. Production and use of H_2 (higher heating value energy content) to 2050 in the E+ RE- scenario.

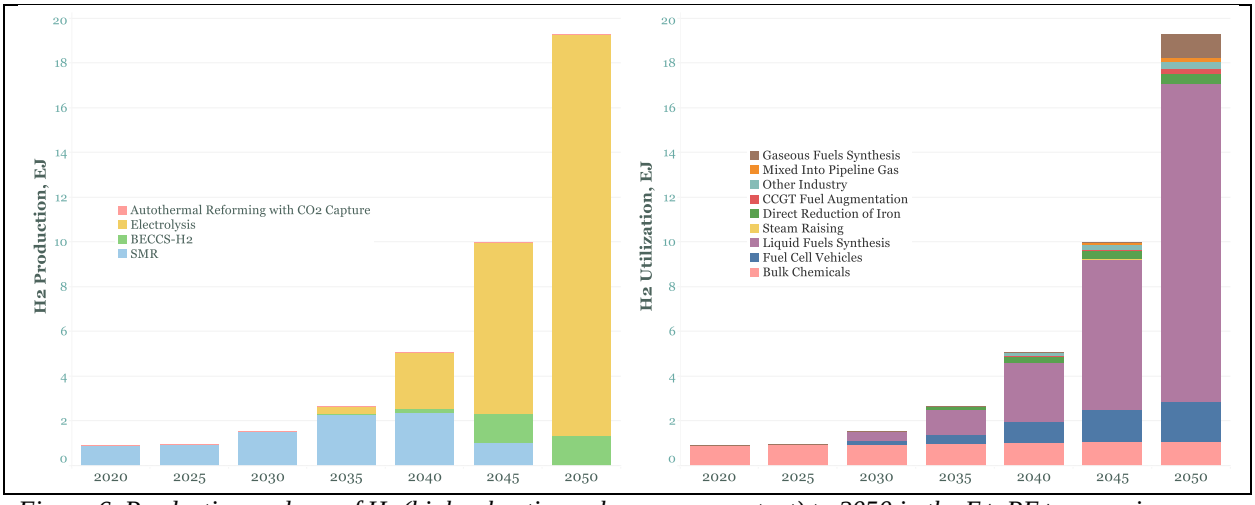

Figure 6. Production and use of H_2 (higher heating value energy content) to 2050 in the E+ RE+ scenario.

For ease of comparison, Figure 7 shows hydrogen production and use in 2050 in each of the five net-zero emissions pathways. Biomass conversion with CO_2 capture stands out as a major supply source in four of the five pathways. This option provides the lowest levelized cost of hydrogen among the three low-carbon hydrogen options, because its negative emissions results in a significant production-cost credit.

For example, in the E+ pathway the marginal price of CO_2 emissions from the energy system, i.e., the system-wide cost of reducing emissions by one more unit of CO_2, reaches \$300/tCO_2 in 2050. (This price reaches up to \$450/tCO_2 in the other pathways.) At \$300/tCO_2, the negative emissions credit for the BECCS-H_2 technology, which captures 135 kgCO_2/$GJ_{H2,HHV}$ (Table 3), amounts to \$5.7/kg. Capital, feedstock, and operating costs in total are about \$4.5/kg (when biomass costs \$100/t). Effectively, therefore, the levelized cost of hydrogen production is negative.

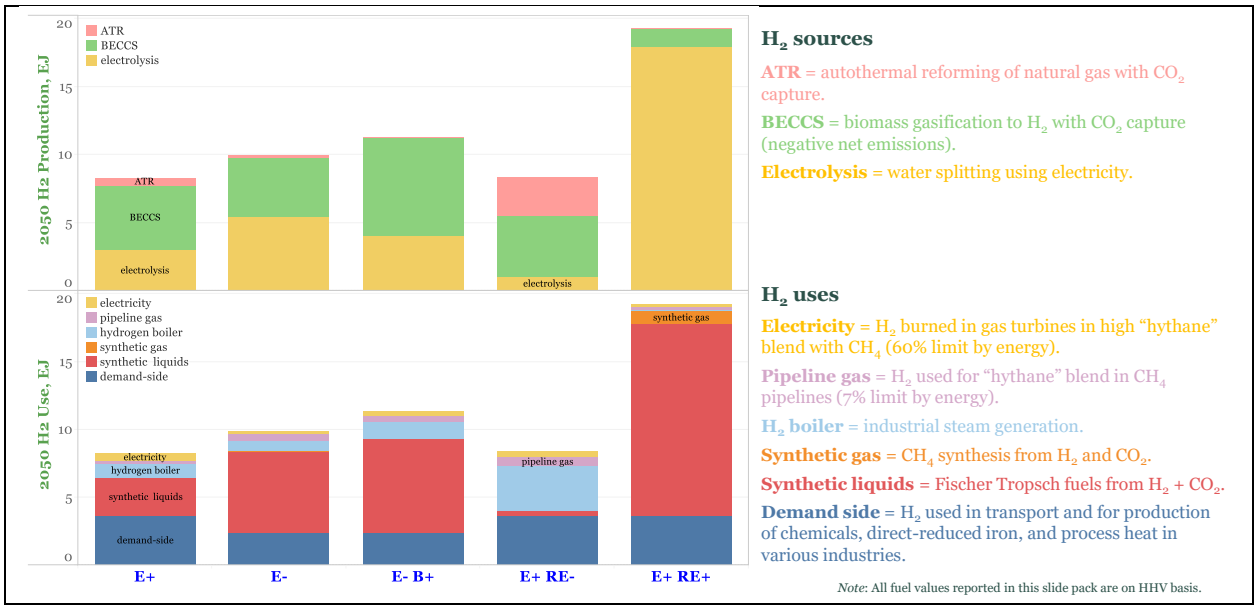

Figure 7. H_2 production and use (higher heating value energy content) in 2050 for each net-zero pathway.

Figure 7 (lower panel) shows that a significant amount of produced H_2 is used for liquid fuels synthesis in most scenarios. Fuels synthesis involves the RWGS-FTS technology (Appendix Table 2) that uses H_2 and captured CO_2 as inputs to produce liquid hydrocarbon fuels that can substitute for petroleum-derived equivalents, such as diesel or jet fuel. The RIO model does not track the origin of H_2 (or CO_2).[†] BECCS-H_2 could be one source of H_2 and/or CO_2 used for fuels synthesis. If BECCS-H_2 were the source for both inputs, it would effectively be mimicking a direct biomass-to-liquids facility with some CO_2 captured for storage (Figure 8). In this case the CO_2 used for liquid fuels production would not be available to be sequestered, and the negative emissions credit for captured/stored CO_2 would be reduced relative to a facility producing merchant H_2 and storing all captured CO_2. The credit would still be substantial, however, corresponding to nearly \$4/kg H_2 produced when the carbon emissions price is \$300/tCO_2. The credit would be sufficient to offset most of the costs of production, making the net cost of BECCS-H_2 still the lowest-cost hydrogen most of the time.

Electrolysis plays an important role by 2050 in all scenarios because the demand for hydrogen exceeds what can be provided by BECCS-H_2 alone under the biomass supply limits imposed in the pathways, even in the E-B+ pathway for which potential biomass supply is much greater than in the other four pathways [8]. In the E+ RE+ pathway, no underground storage of CO_2 is allowed, so BECCS-H_2 does not benefit from any negative emissions credit. This makes BECCS-H_2 a less competitive hydrogen option and leads to electrolysis dominating hydrogen supply in this pathway (Figure 7).

[†] RIO mixes all produced H_2 into a single stream from which H_2 is withdrawn for different uses. Similarly, RIO mixes all captured CO_2 into a single stream from which CO_2 is withdrawn for fuels synthesis or underground storage.

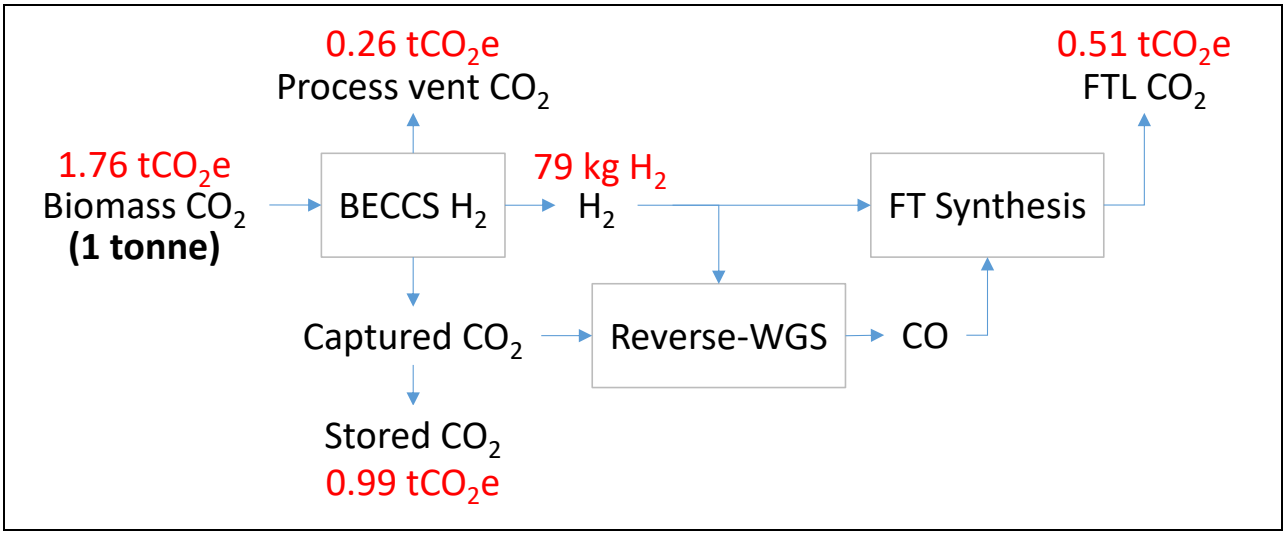

Figure 8. Carbon balance for fuels synthesis using H_2 and CO_2 from BECCS-H_2. The amount of CO_2 needed to convert all of the H_2 from the BECCS- H_2 unit to Fischer-Tropsch liquid fuel (FTL) is less than the total amount captured; some of the captured CO_2 is stored and provides negative emissions.

2.2. Coarse geographic distribution of hydrogen producers and users

The RIO model balances hydrogen production and consumption on an annual basis within each of 14 model regions representing the continental U.S. Regional distributions of production and use are shown for the E+ scenario in 2050 in Figure 9. Production is dominated by biomass-derived H_2 in the Upper Midwest, Mid-Atlantic/Great Lakes, Southeast, and Louisiana/Ozarks regions. Texas and California are notable for ATR-CC deployments, and electrolysis plays a role in all regions, with the most significant contributions in the Upper Midwest, New England, and New York.

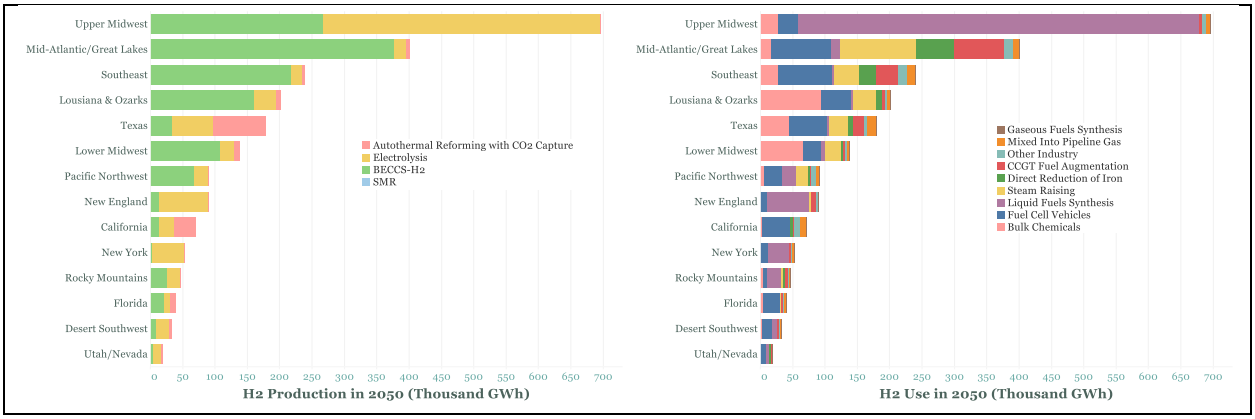

Figure 9. Regional distribution of H_2 production and use in 2050 in the E+ pathway.

Similar distributions of producers and users are observed for the E- pathway (Figure 10) and the E- B+ pathway (Figure 11), with the Upper Midwest and Mid-Atlantic/Great Lakes regions standing out still further. In the E+ RE- pathway, because of the greater reliance on natural gas derived hydrogen, there is a broader geographical distribution of production and utilization, with industrial steam production being the dominant use for hydrogen as a replacement for natural gas (Figure 12). There is also broader geographical distribution in the E+ RE+ pathway (Figure 13),

where electrolysis is the dominant source. The dominant use in this pathway is synthetic fuels production, given the constraint that fossil-derived liquid fuels are completely eliminated by 2050. Unlike hydrogen, which the model constrains to be used in the region it is produced, liquid fuels synthesized using hydrogen are allowed to be moved between regions in order to meet aggregate national liquid fuel demands.

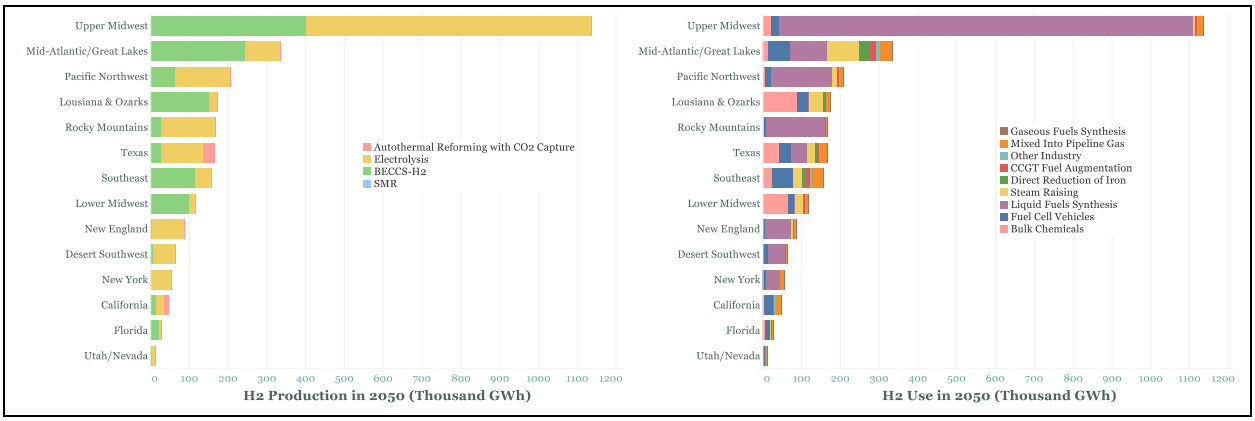

Figure 10. Regional distribution of H_2 production and use in 2050 in the E- pathway.

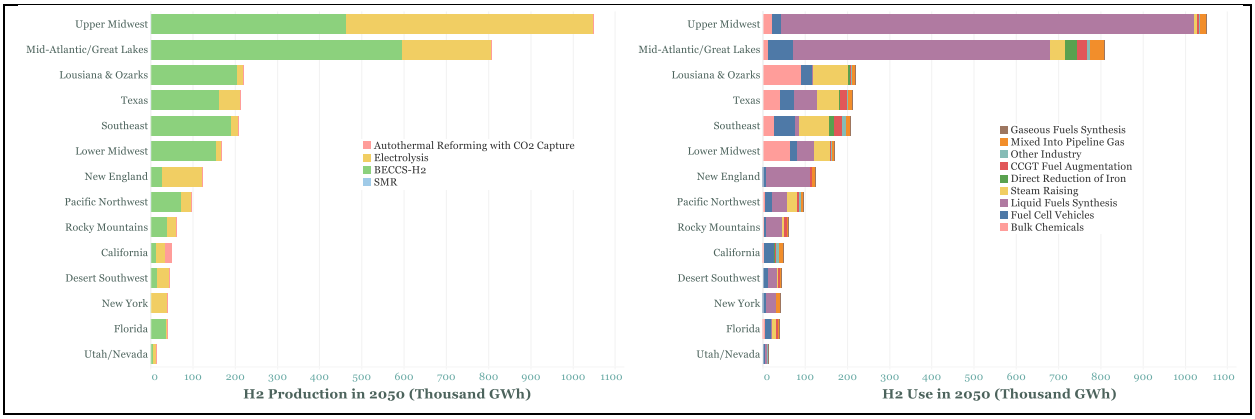

Figure 11. Regional distribution of H_2 production and use in 2050 in the E- B+ pathway.

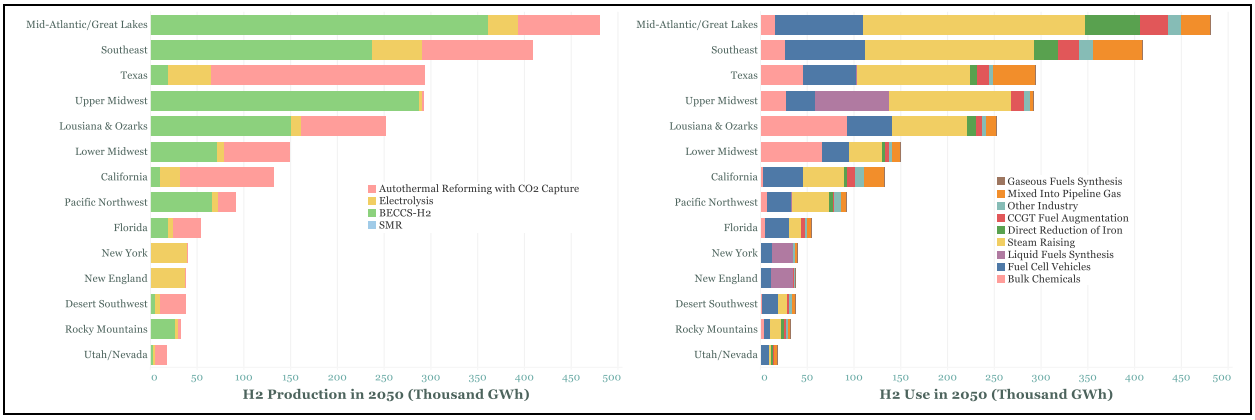

Figure 12. Regional distribution of H_2 production and use in 2050 in the E+ RE- pathway.

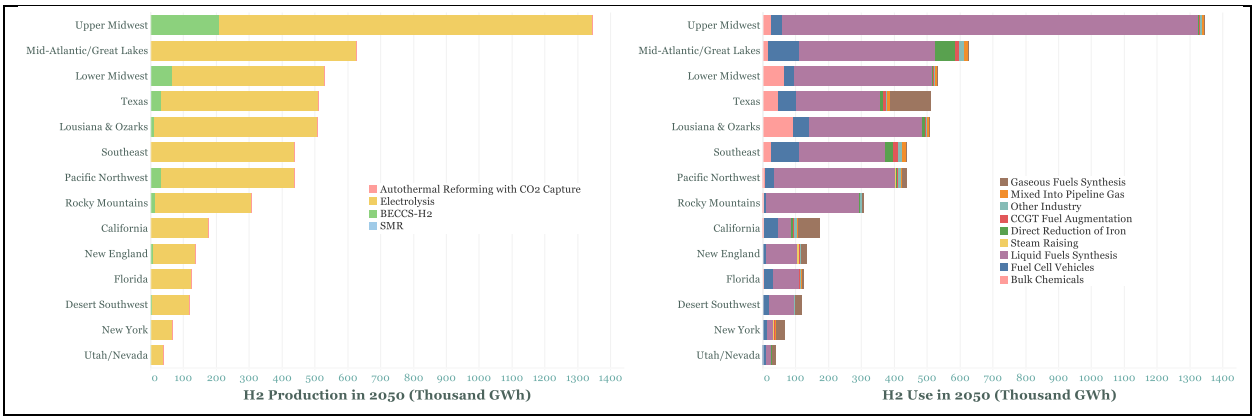

Figure 13. Regional distribution of H_2 production and use in 2050 in the E+ RE+ pathway.

2.3. Notional downscaled siting of hydrogen producers and users

Finer-resolution mapping of hydrogen production and utilization, beyond the 14 regions discussed above, was not undertaken in our study in the way that downscaling was for some other features of the net-zero pathways, including solar and wind electricity generators [9], biomass supply and conversion sites [8], and CO_2 transport and storage infrastructure [10]. Future work at Princeton is planned to evaluate hydrogen production and use at finer spatial scales.

Without the benefit of finer-scale geospatial analysis, however, a general idea of how hydrogen production might be located relative to users can be developed. For illustration, we consider the E+ pathway. On the production side, H_2 from biomass accounts for nearly 60% of supply in 2050. Siting of these production facilities will be constrained primarily by where the biomass is produced, due to relatively high costs of biomass transport. By comparison, electrolysis, accounting for 35% of production in 2050, has more flexibility in siting, since the primary constraint is proximity to high-voltage transmission. Siting of ATR, which accounts for the remaining 7% is also relatively unconstrained, since the natural gas transmission network in the U.S. is extensive.

For siting of hydrogen users, their diversity requires considerations specific to each use. Considering the E+ pathway for illustrative purposes, we can note that in 2050:

- About 1/3 of hydrogen demand is for synthesis of liquid fuels, which requires both H_2 and CO_2 as feedstocks. Given the availability of both of these at BECCS-H_2 facilities, the majority of RWGS-FTS plants might be co-located with BECCS-H_2 facilities. The stoichiometry of fuels synthesis is such that only about one-third of the CO_2 captured at a BECCS-H_2 facility would be needed to convert all the H_2 produced at that facility to synthetic fuels, so the balance of the captured CO_2 would be stored underground via injection into a nearby storage formation or after delivery by pipeline to a distant storage site. If co-locating RWGS-FTS with BECCS-H_2 is not possible in a particular region for some reason, the RWGS-FTS facility might be co-located with either electrolysis or an ATR-CC facility proximate to a CO_2 pipeline.
- About 20% of hydrogen is for fuel cell vehicles. Options for this H_2 supply could include onsite hydrogen production via ATR-CC or electrolysis at large refueling stations or truck-delivered H_2 (from biomass, ATR-CC, or electrolysis) for smaller stations.

- Finally, the approximately 7% of H_2 injected into the gas pipeline network might be produced by any of the three production options if located near the gas pipeline system.
- The largest share of hydrogen, about 40%, goes to industrial uses, including for bulk chemicals production, direct reduction of iron, various other distributed industrial users, and to augment natural gas at gas turbine power plants. Many such industries will have access to the pipeline gas used as input to ATR-CC and might have the capability to install and operate a thermochemical process like ATR-CC with CO_2 capture. For relatively small and distributed industrial users, however, electrolytic H_2 production might be preferred. The modularity of the technology and its siting flexibility would lend themselves to this. For industries where onsite H_2 production is not feasible, regional clusters of industrial hydrogen users might share a H_2 pipeline network supplied by H_2 from biomass, ATR-CC, and/or electrolysis.

2.4. Regional hydrogen pipeline system vignettes

To help better envision what future regional H_2 production and use systems might look like, we sketch here some notional hydrogen pipeline networks for six specific regions in the U.S. (Figure 14).

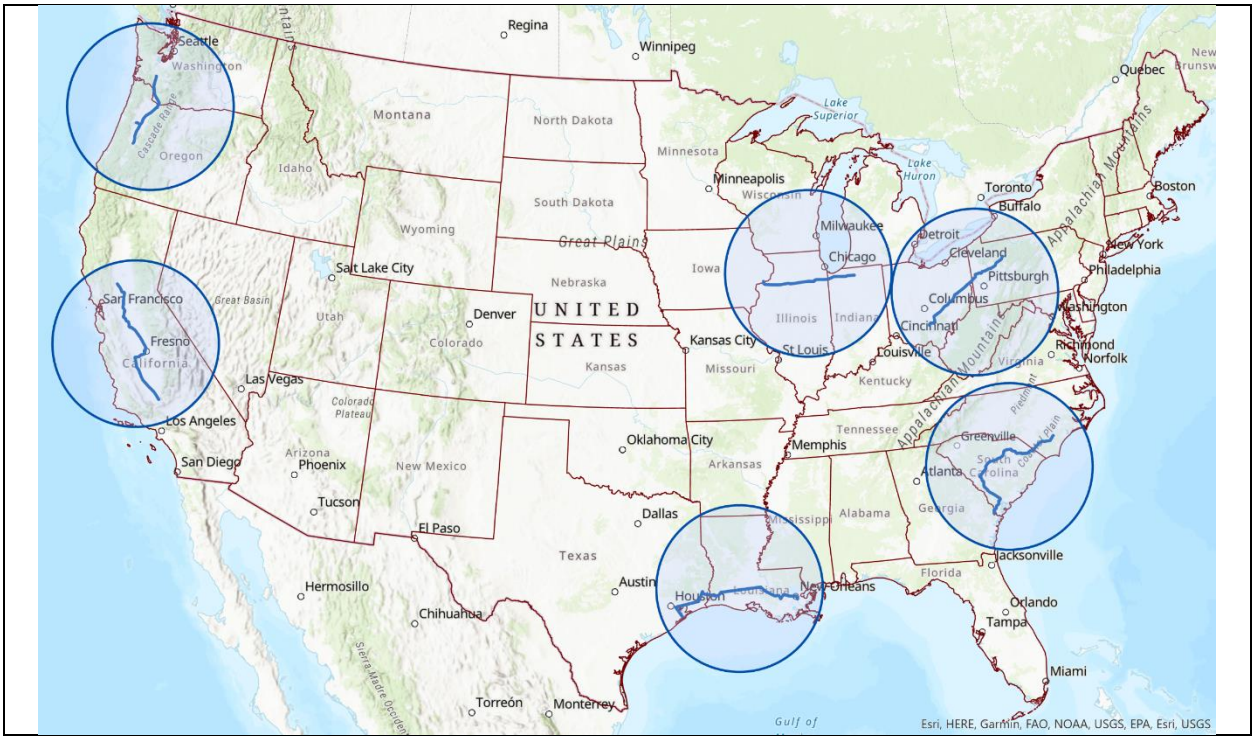

Figure 14. Circles (each having a radius of 200 miles) indicate regions for which notional hydrogen trunk and spur pipeline systems have been sketched in the Annex (Figure 16, Figure 17, Figure 18, Figure 19).

More than half of the total of about 4,500 km of hydrogen pipelines operating in the world as of 2016 are in the U.S. [11], with more under development [12]. Thus, there are precedents that can help with envisioning future systems. Conceptually, regional hydrogen pipeline systems serving industrial users might resemble those operated in the U.S. today by Air Products & Chemicals [13], Air Liquide [14], and Praxair [15]. Figure 15 shows the Air Products Gulf

Coast hydrogen pipeline system, including hydrogen production facilities that feed the pipeline. Users of hydrogen are distributed up and down the full 600-mile extent of the pipeline system.

Inspired by the layout of the Air Products Gulf Coast hydrogen pipeline system, Figure 16 sketches a notional hydrogen trunk and spur pipeline system connecting hypothetical hydrogen production facilities with hypothetical industrial users in the 2050 E+ scenario. Hydrogen is produced from biomass or natural gas with CO_2 capture and fed to a variety of industrial users.

Figure 17, Figure 18, and Figure 19 show additional notional hydrogen pipeline systems that might serve industrial users in other regions of the U.S. in 2050 under the E+ scenario.

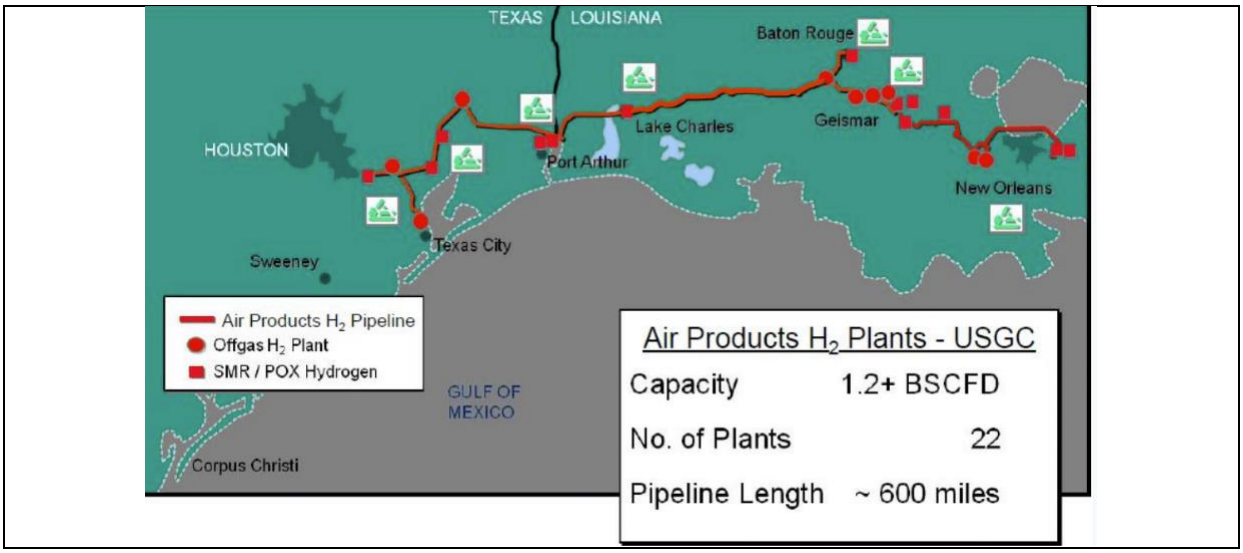

Figure 15. Existing U.S. Gulf Coas Air ProductsH_2 production and delivery infrastructure [16].

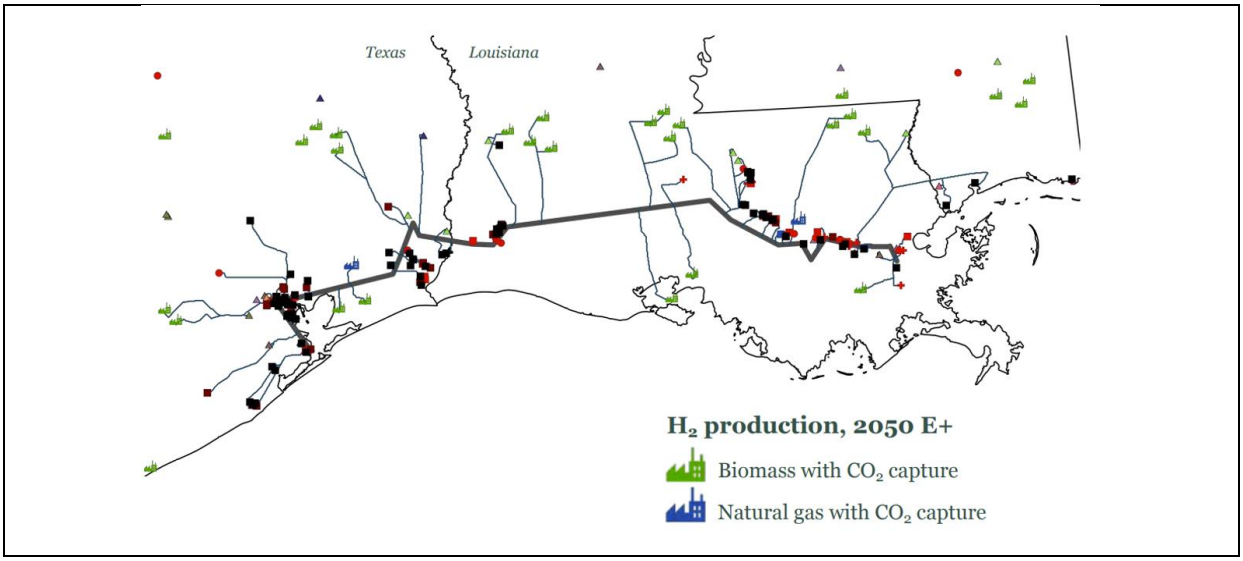

Figure 16. Notional hydrogen trunk and spur pipeline system connecting hypothetical hydrogen production facilities with hypothetical industrial users. The locations of biomass-H_2 production sites (green-factory icons) are based on bioconversion plant siting analysis for 2050 in Annex H [8]. The natural gas-based H_2 production units (blue-factory icons) have been arbitrarily sited for illustrative purposes. Industrial hydrogen users (squares, circles, triangles and plus signs) are indicated where facilities today (2017) are producing bulk chemicals, refined petroleum products, iron and steel, and other products [17]. See Appendix B for a summary of the methodology used to visualize the H_2 pipeline system

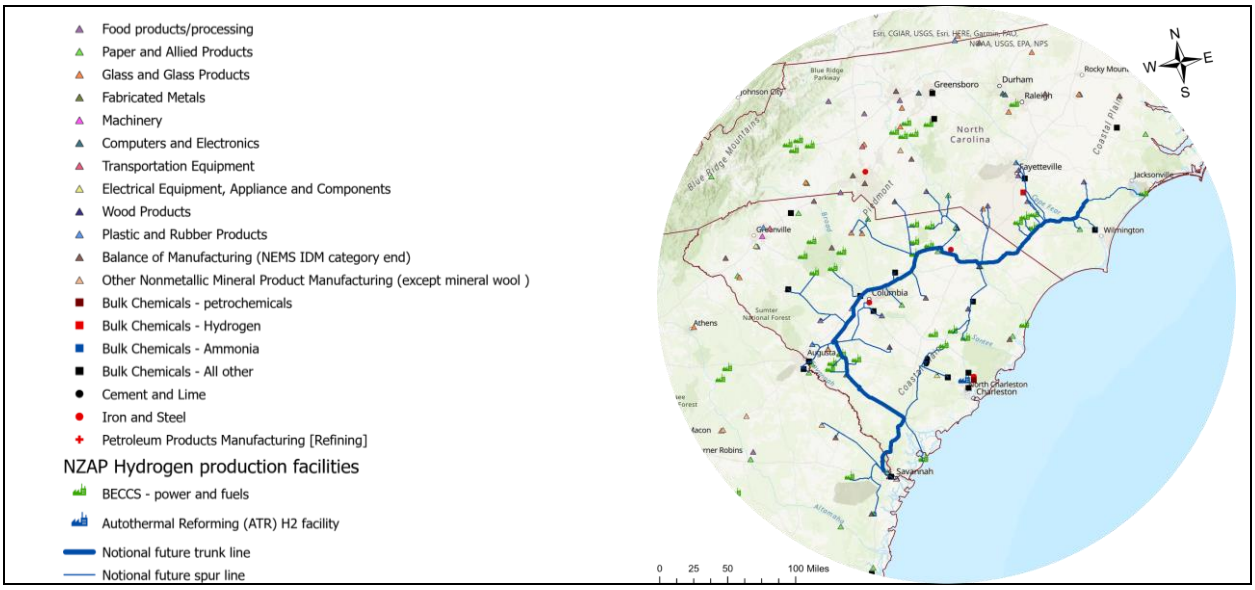

Figure 17. Notional hydrogen trunk and spur pipeline system connecting hypothetical H_2 production facilities with hypothetical industrial H_2 users in a region of the Southeastern U.S. H_2 users are located where industrial facilities exist today emitting 25,000 tonnes of CO_2 per year or more [17]. See Appendix B for a summary of the methodology used to visualize the H_2 pipeline system.

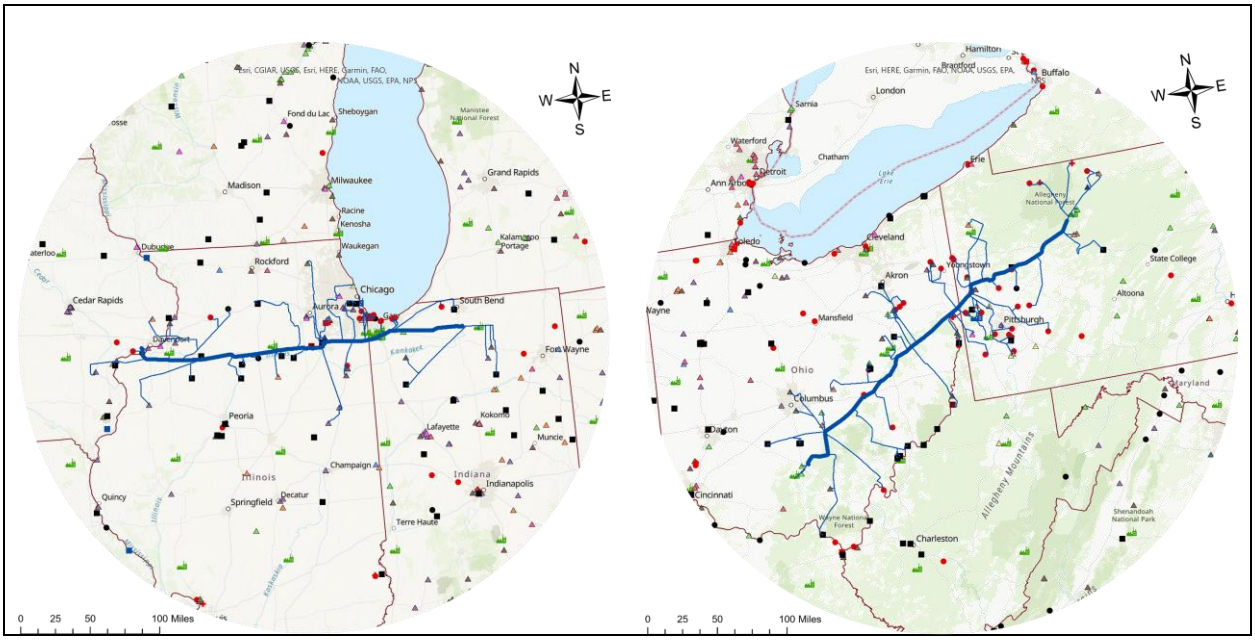

Figure 18. Notional hydrogen trunk and spur pipeline system connecting hypothetical H_2 production facilities with hypothetical industrial H_2 users in Northern Illinois and Indiana (left) and in Ohio and Western Pennsylvania (right). H_2 users are located where industrial facilities exist today emitting 25,000 tonnes of CO_2 per year or more [17]. See Figure 17 for map legend. See Appendix B for a summary of the methodology used to visualize the H_2 pipeline systems.

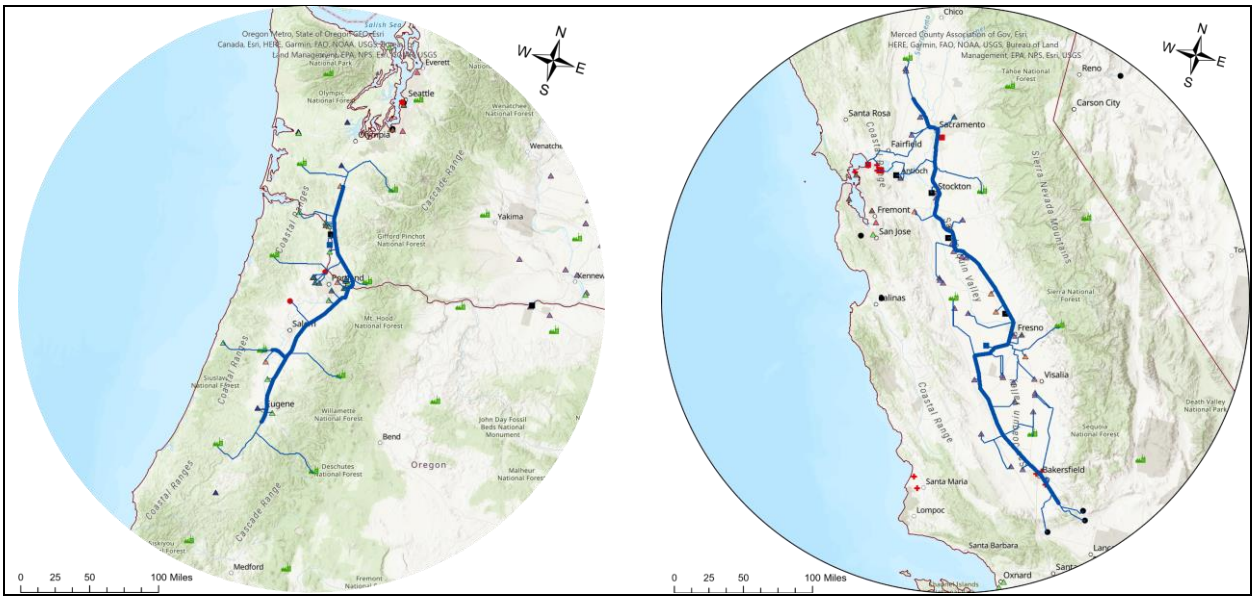

Figure 19. Notional hydrogen trunk and spur pipeline system connecting hypothetical H_2 production facilities with hypothetical industrial H_2 users in Southern Washington and Northern Oregon (left) and in California's Central Valley (right). H_2 users are located where industrial facilities exist today emitting 25,000 tonnes of CO_2 per year or more [17]. See Figure 17 for map legend. See Appendix B for a summary of the methodology used to visualize the H_2 pipeline systems.

Appendix A: Technology Performance and Cost Assumptions

Performance and cost estimates for most of the technologies found in the RIO model for converting biomass, natural gas, or electricity to liquid or gaseous hydrocarbon fuels, as well as those for converting biomass to electricity with CO_2 capture, are documented in this Appendix. These estimates are based on detailed publicly available studies of N^{th} plant designs, i.e., studies that assume technology performance and cost have reached commercially mature (N^{th} plant) levels. An underlying assumption in the RIO model is that each technology will have been developed to this point by the first date that RIO has the option of deploying that technology. For example, this date is 2030 in the case of ATR-CC and 2035 in the case of BECCS-H_2.

Recognizing that there are considerable uncertainties in future performance and cost estimates, we assume in all but one case that the estimated N^{th} plant estimates remain at their initial values for the entire transition period: no performance improvements or cost reductions are assumed to occur. The only exception to this is for electrolysis, for which cost reductions are expected over time [18,19] because, unlike the other technologies described here, the modular nature of electrolysis lends itself to the type of cost learning that has been observed in practice for solar PV modules and wind turbines [20], as well as lithium-ion batteries [21]. In this appendix:

- Table 1 provides reference energy and carbon contents of fuels.
- Table 2 details performance and cost estimates for liquid fuels production technologies.
- Table 3 details performance and cost estimates for hydrogen production technologies.
- Table 4 details performance and cost estimates for biomass-gasifier power generation.
- Table 5 details modeling assumptions for hydrogen storage and delivery.

Table 2, Table 3, and Table 4 show parameter values used in the RIO model. There are small discrepancies in some cases between these values and the values derived from the literature as explained in the table notes. The discrepancies are negligible considering the level of uncertainty inherent in the performance and cost estimates.

Table 1. Energy and carbon contents of fuels.

	HHV, GJ/t	HHV/LHV	Carbon content, kg CO_2e/GJ_{HHV}
Biomass	19.8	1.07	88.9
Methane	55.5	1.11	50
Hydrogen	142	1.18	0
FTL	45.5	1.05	67.2

Table 2. Performance and cost estimates for liquid fuels production technologies.

Technology	Inputs & co-products (all HHV basis)		CO_2 captured or input,[a] kg CO_2 / $GJ_{liq\ fuel,HHV}$	Installed capital cost,[b] $\$_{2016}$ / $kW_{liq\ fuel,HHV}$	Fixed O&M,[b] $\$_{2016}/kW_{liq\ fuel,HHV}$-yr	Variable O&M[b] $\$_{2016}/GJ_{liq\ fuel,HHV}$
	Input, $GJ/GJ_{liq\ fuel}$	Co-product, $GJ/GJ_{liq\ fuel}$				
Biomass to FTL (BioFT)[c]	1.96 (biomass)	0	0	4,215	204	5.4
BioFT w/cc[c]	1.96 (biomass)	0	- 85	4,387	207	6.7
Pyrolysis (BioPyr)[d]	1.54 (biomass)	0.117 (electricity)	0	2,491	98	5.2
BioPyr w/cc[d]	1.54 (biomass)	0.028 (electricity)	- 78	3,992	156	5.2
RWGS-FTS[e]	1.47 (H_2)	0	68	952	28	0.6

(a) Negative values indicate CO_2 captured. Positive values indicate CO_2 input.

(b) All costs are expressed in 2016 $, the dollar-year for inputs to the energy-system modeling described in Annex A. To convert costs to 2016 $ from other dollar years in the original literature sources, the Chemical Engineering Plant Cost Index, GDP deflator, or other indices were applied.

(c) Parameters for biomass-to-FTL technologies are based on [22], which reports the following for a facility converting woody wastes to FTL: FTL output capacity of 290 MW FTL_{LHV}; biomass input capacity of 600 MW_{LHV}. Additionally, for BioFT and BioFT w/cc, respectively: total installed capital cost in 2017 € of 1200 M $€_{2017}$ and 1222 M $€_{2017}$; fixed O&M costs (assuming 8,000 hours/yr operation) of 6.9 $€_{2017}/GJ_{FTL,LHV}$ and 7 $€_{2017}/GJ_{FTL,LHV}$; and variable O&M costs of 4.9 $€_{2017}/GJ_{FTL,LHV}$ and 6.1 $€_{2017}/GJ_{FTL,LHV}$. For BioFT w/cc, approximately 70% of the carbon input as biomass and not converted to FTL is assumed to be captured. HHV:LHV ratios (Table 1) were used to express biomass and FTL quantities on a HHV basis here, and an exchange rate of 1.1 $/€ (average for 2017) was assumed.

(d) Parameters are based on two process configurations of a catalytic hydropyrolysis technology described in [23]. One configuration has no CO_2 capture and the other is with maximum CO_2 capture. Each has a biomass input rate of 687 MW_{LHV} and liquid fuels output rate of 446 MW_{LHV}. Electricity is co-produced in each case: 55 MW_{el} and 13 $MW_{el,}$ respectively, without and with carbon capture. Annual fixed O&M is 4% of the installed capital cost. The variable O&M cost is the sum of catalyst cost (4.87 $\$_{2014}$/t biomass) and refining cost (4.51$\$_{2014}/GJ_{FTL,LHV}$). Ratios of HHV to LHV (Table 1) were used as needed to convert to HHV amounts. Estimated installed capital costs are 1224 M $\$_{2014}$ and 1990 M $\$_{2014}$, respectively, for the designs without and with CO_2 capture. For the design with CO_2 capture, 94% of the biomass carbon not contained in the liquid fuels is captured.

(e) This process uses reverse water-gas shift (RWGS) followed by Fischer-Tropsch synthesis (FTS) to convert input H_2 and CO_2 into refined synthetic diesel, jet fuel and LPG. (In Annex A, this technology is referred to as "power-to-liquids" because one possible source of the H2 input is electrolysis.) The following calculations were used to estimate the H_2 input required per unit of FTL output. FTS, which synthesizes liquids from H_2 and CO, requires a fresh syngas feed of 2 moles of H_2 for each mole of CO. From Table 4 and Figure 12 in Greig *et al.* [24], a "once-through" FT synthesis configuration, *i.e.*, with no internal recycle of unconverted syngas or reformed light-ends, will produce 76.2 MJ/s (LHV) of liquid fuels from a fresh syngas feed containing 0.79 kg/s of H_2 (0.395 kmol/s) and 5.49 kg/s of CO (0.196 kmol/s). With internal recycle, the liquid fuels output increases 43% for the same syngas input (based on comparing outputs in Table 17 of [24] for case RC-0 and OT-0). Thus, the H_2 flow in the input syngas corresponds to 0.79 kg/s * 142 MJ_{HHV}/kgH_2 = 112 $MJ_{H2,HHV}$/s, or 112 / (76.2*1.43*1.05) = 0.98 MJ_{HHV} of H_2 per MJ_{HHV} of FT fuels (using HHV:LHV for FT fuels from Table 1). Additional H_2 input is needed for the RWGS used to produce CO from CO_2. RWGS requires 1 kmol of H_2 to produce 1 kmol of CO ($H_2 + CO_2 \rightarrow CO + H_2O$), so the overall H_2 requirement for the RWGS-FTS process is 3 kmol of H_2 for each kmol of CO_2. Thus, the total H_2 required is: (3/2)*0.98 = 1.47 $MJ_{H2,HHV}/MJ_{HHV,FTL}$. The installed capital cost is derived from the cost for the system design labeled RC-B in Table 17 of [24]. The FTL output capacity is the sum of liquid outputs for this design: 239 $MW_{FTL,LHV}$ or 251 $MW_{FTL,HHV}$. The installed capital cost is approximated by summing the costs of two line items from Table 19 of [24], FT synthesis + refining and light ends processing, and a balance-of-plant cost estimated as the sum of line items GT, HRSC and BOP multiplied by the fraction of syngas converted to liquids in the RC-B design. No explicit cost is included for the RWGS process, because the RC-B design in [24] includes the cost for a water gas shift reactor. This results in an estimated total capital cost for the RWGS-FTS process of 244 $M\$_{2015}$, which converts to the unit capital cost estimate shown here. Fixed and variable O&M costs for the RWGS-FTS process is based on Capros *et al.* [25]. In our modeling, fixed O&M costs are assumed to decrease over time, reaching the value shown here by 2050.

Table 3. Performance and cost estimates for hydrogen production technologies in RIO modeling.[a]

	Inputs & Co-products (all HHV basis)		CO_2 captured (kg CO_2/ $GJ_{H2.HHV}$)	Installed capital cost[c] ($\$_{2016}$/kW $H_{2\ HHV}$)[c]	Fixed O&M[c] ($\$_{2016}$/kW H_{2HHV} - yr)	Variable O&M[c] ($\$_{2016}$/GJ $H_{2\ HHV}$)
	Main input (GJ/GJ_{H2})	Co-product[b] (GJ/GJ_{H2})				
BECCS-H_2 [d]	1.78 (biomass)	- 0.027 (electricity)	135	2,599	18	3.2
ATR w/cc[e]	1.20 (natural gas)	0.048 (electricity)	52	782	20	0
Electrolysis[f]	1.28 (electricity)	0	0	550	30	0.083

(a) The RIO model was constrained such that commercial deployment is not allowed until 2030 for ATR w/cc and 2035 for BECCS-H_2. Cost and performance for these technologies are assumed constant through 2050 at the values shown here. Deployment of electrolysis is allowed in any time step, and its costs are assumed to fall and performance assumed to improve with time, reaching the values shown here in 2050.

(b) Positive values are co-products. Negative values are required inputs.

(c) All costs are expressed in 2016 $, the dollar-year for inputs to the energy-system modeling described in Annex A. To convert costs to 2016 $ from other dollar years in the original literature sources, the Chemical Engineering Plant Cost Index, GDP deflator, or other indices were applied.

(d) The BECCS-H_2 estimates are based on Davison *et al.*'s assessment of a variety of coal-gasification based process configurations for co-production of hydrogen and electricity [26]. Values in this table are derived from Davison's cases 5.3 and 4.2. Among all of Davison's configurations, Case 5.3 produces the highest fraction of hydrogen in the outputs (97.4%), with electricity constituting the balance. Case 4.2 produces the lowest fraction (0), i.e., it produces electricity only. We assume that the ratio of performance and cost parameters between the two cases would be the same if the plants were designed for biomass instead of coal. We scale the performance and cost estimates for the biomass-gasifier combined cycle plant with CO_2 capture described in Table 4 using ratios of parameter values from Davison's Case 5.3 and 4.2 to estimate performance and costs for a BECCS-H_2 plant.
- Case 4.2 power output = 874.3 MW_{el}; Case 5.3 power output = 37 MW_{el}; Ratio = 874.3 / 37 = 23.6
- Case 5.3 H_2 output / electricity output = 1,390 $MW_{H2,LHV}$ / 37 MW_{el} = 37.6
- The ratio of total plant cost for Case 5.3 to Case 4.2 = 2,101 M €$_{2013}$ / 2,688 M €$_{2013}$ = 0.78.
- The ratio of annual fixed O&M costs for Case 5.3 to case 4.2 = 90,210,200 €$_{2013}$ / 112,520,000 €$_{2013}$ = 0.80.
- The ratio of annual variable O&M costs for Case 5.3 to case 4.2 = 8,918,700 €$_{2013}$ / 9,752,700 €$_{2013}$ = 0.91.
- BECCS-H_2 characteristics are, therefore:
  - power output = BECCS-el output * (Case 5.3 / Case 4.2) = 214 MW_{el} / 23.6 = 9.06 MW_{el}
  - H_2 output = 9.06 MW_{el} * (Case 5.3 H_2/power) = 9.06 * 37.6 = 341 $MW_{H2,LHV}$ (or 400 $MW_{H2,HHV}$)
  - biomass input / H_2 output = 711 $MW_{bio,HHV}$ / 400 $MW_{H2,HHV}$ = 1.78 $MW_{bio,HHV}/MW_{H2,HHV}$.
  - electricity input / H_2 output = 9.06 / 400 = 0.023 $MW_{bio,HHV}/MW_{el}$. The RIO data base uses 0.027, but overall RIO results are not materially impacted by this slightly higher value.
  - the fraction of input biomass carbon captured is assumed to be the same as for a BECCS facility producing electricity only (see Table 4). This gives a CO_2 capture rate of 135 $kgCO_2/GJ_{H2,HHV}$.
  - total plant cost (TPC) is estimated as the product of TPC for BECCS-el [$1,171, Table 4 note (b)] and the ratio of Case 5.3 to Case 4.2 TPC: 1,171 * 0.78 = 915 M $\$_{2018}$. We add owners costs to get a total estimated installed capital cost for BECCS-H_2 of 1,083 M $\$_{2018}$, or 2,708 $\$_{2018}/kW_{H2,HHV}$.
  - annual fixed O&M is the value for BECCS-electricity multiplied by the ratio of fixed O&M for Davison case 5.3 and case 4.2. Fixed O&M for BECCS-el (from Table 4) is 108 $\$_{2016}$/kW-yr * 214 MW_{el} = 23.1 M $\$_{2016}$. Thus, fixed O&M for BECCS-H_2 = 23.1 M $\$_{2016}$ * 0.80 /400 $MW_{H2,HHV}$ = 46 $\$_{2016}$/kW-yr. The RIO modeling erroneously used 18 $\$_{2016}$/kW-yr, but overall energy-system model results would not be materially different if the higher value had been used.
  - annual variable O&M is the value for BECCS-electricity multiplied by the ratio of annual O&M for Davison case 5.3 and case 4.2. Variable O&M for BECCS-el (from Table 4) is 23.6 $\$_{2016}$/MWhr * (214 MW_{el} * 8760 * 0.9) = 39.8 M $\$_{2016}$. Thus, variable O&M for BECCS-H_2 = 39.8 M $\$_{2016}$ * 0.91 / (400 $MW_{H2,HHV}$ * 8760 h/y * 0.9 CF) = 11.4 $\$_{2016}$/MWh, or \$3.2/$GJ_{H2,HHV}$.

(e) Performance and capital cost estimates for autothermal reforming of methane with CO_2 capture are based on Table 3.13 in [7] for a 1.5 GW_{H2} capacity facility. The installed capital cost estimate of 631 £$_{2017}$/$kW_{H2,HHV}$ was converted to $ using the average £/$ exchange rate in 2017 (1.29) and adjusting to 2016 $. The annual fixed O&M cost is 3% of installed capital cost. Variable operating costs are neglected.

(f) For electrolytic H_2 production, the assumed efficiency of 78% is based on [27] and assumed to be the same throughout the transition period. Costs in this table use [28] as a guideline. The assumed capital cost for 2050 is shown. Costs fall to this level through the transition period, starting from a value of 1790 $\$_{2016}/kW_{H2,HHV}$ in 2020.

Table 4. Performance and cost estimates for biomass-gasification-based power generation.

	$Energy_{in}/Energy_{out}$ (all HHV basis)					
	Main input (GJ_{bio}/GJ_{el})	Co-product (GJ/GJ_{el})	CO_2 captured ($kgCO_2/MWh_{el}$)	Installed capital cost[a] ($\$_{2016}$/kW)	Fixed O&M[a] ($\$_{2016}$/kW- y)	Variable OM[a] ($\$_{2016}/MWh_{el}$)
BECCS-el[b]	3.32	0	990	6,338	108	24
Bio-Allam[c]	2.48	0	796	7,144	231	24

(a) All costs are converted to 2016 $, the dollar-year for inputs to the energy-system modeling described in Annex A. To express costs in 2016 $ from other dollar years, the Chemical Engineering Plant Cost Index, GDP deflator, or other indices were applied.

(b) The BECCS-electricity parameters are based on the case identified as SB95-B in Kreutz *et al.* [29], which includes pre-combustion CO_2 capture. In this plant design, biomass is gasified and the resulting syngas is subjected to cleaning, water gas shift, and Rectisol CO_2 removal, after which 95% of the hydrogen-rich syngas goes to fuel a gas turbine combined cycle. The remaining 5% is converted via Fischer-Tropsch synthesis to hydrocarbon liquids. The biomass input rate is 711 $MW_{bio,HHV}$. The net electricity output for this plant is 194.3 MW_{el}. We estimate that if 100% of the syngas were used for power generation, net electric power output would increase to 214 MW_{el} for the same biomass input level (711 $MW_{bio,HHV}$), and the CO_2 capture rate would be 990 $kgCO_2$/MWh (87% of input biomass carbon captured). Kreutz, *et al*. estimate a total plant cost (TPC) for SB95-B of 1515 M $\$_{2018}$. Accounting for differences between the SB95-B configuration and a 100% electricity generating configuration, we estimate a TPC of 1,171 M $\$_{2018}$ for the latter, to which we add owner's costs, resulting in a total installed capital cost of 1,386 M$\$_{2018}$, or 6,477 $\$_{2018}/kW_{el}$. Kreutz *et al*. indicate a 90% capacity factor for SP95-B and total annual O&M costs of 5.5% of TPC. O&M costs for the 100% electricity plant are therefore estimated to be 38 $\$_{2018}$/MWh (= 1,171 M $\$_{2018}$ * 0.055 / [214.2 * 8760 *0.9]). We assume that non-fuel variable O&M costs are 63% of this total, based on detailed estimates for coal-gasification based electricity plant designs with CO_2 capture using GE quench gasifier [30]. Thus, variable O&M costs are 24 $\$_{2018}$/MWh and fixed operating costs are 14 $\$_{2018}$/MWh, or 108 $\$_{2018}$/kW-yr.

(c) This is a biomass-gasifier Allam cycle that captures as CO_2 essentially all input biomass carbon. Efficiency and CO_2 capture rate are as estimated for a fluidized-bed lignite-gasifier Allam cycle in Laumb [31]. The unit installed capital cost estimate is also from [31], but has been adjusted by the inclusion of owners costs as part of installed capital cost. Laumb reports total annual O&M costs to be 3.2% of the installed capital cost. Conservatively, we assume this level for fixed O&M costs and assume variable O&M costs are as estimated for BECCS-el.

Table 5. Hydrogen delivery and storage assumptions [32].

H_2 delivery and use	- H_2 production and use must balance in each of the 14 RIO model regions at each modeled time step. - The production and use of liquid fuels synthesized from H_2 and CO_2 must balance nationally at each modeled time step, but liquid fuels produced in one RIO model region may be used in a different region. - H_2 demands are divided into two categories for purposes of assigning delivery costs from production to point of use: H_2 for fuel cell vehicles and H_2 for all other uses. Fuel cell vehicle H_2 is assumed to be compressed to a liquid and delivered by truck, with compression losses and electricity use of 39.5 $kWh_{H2,HHV}$ and 8.98 kWh per kgH_2 delivered, respectively. Truck delivery adds \$1.18 $\$_{2005}$ per kgH_2 delivered. For all other H_2 uses, delivery costs are neglected, implying that production will most often be co-located with use.
H_2 storage	- RIO deploys optimal build of H_2 storage and tracks state-of-charge for 365 days yearly. - H_2 storage capital costs are estimated based on above-ground tank storage. Capital costs in 2050 are assumed to be 4,660 €/$MWh_{H2,HHV}$, or about 1,400 $\$_{2016}/GJ_{H2,HHV}$, with an economic life of 20 years.

Appendix B: Visualization of Hypothetical Regional H_2 pipelines

The notional hydrogen pipeline visualizations where generated using the following steps for each of the six regional "vignettes" constructed:

A. Place the green BECCS-H_2 facility icons in locations determined in the analysis in Annex H.
B. Represent industrial H_2 users with facilities from the EPA's Facility Level GHG emissions dataset [17] [reporting year = 2017; No GHG filter]. Choose a facility's icon color/shape by mapping its NAICS code [33] (provided in [17]) into the corresponding industry category as identified in the *Annual Energy Outlook* [34].
C. Select notional endpoints by eye for the H_2 trunk pipeline based on local/regional synergistic groupings of H_2 producers and users.
D. Generate a H_2 pipeline routing surface by preferencing the use of existing natural gas pipeline corridors [35], while penalizing the crossing of all the same environmental / conservation / recreation features excluded in the siting of wind turbines (see Annex D for a full list of exclusion types). Allow routing of H_2 pipelines in exclusion areas if it follows an existing natural gas pipeline right of way through that exclusion area.
E. Use the H_2 routing surface to connect the two endpoints of the trunk line (step C) along the shortest route, while following existing natural gas pipeline corridors as much as possible. The exception to this step is the gulf pipeline, for which we placed the H_2 trunk line to follow essentially the same routing as an existing H_2 pipeline in that region [13].
F. For regions in which the NZA modeling results include H_2 supply from autothermal reforming of natural gas with CO_2 capture (ATR-H_2), place at arbitrary locations on the trunk line blue factory icons representing ATR-H_2 production plants.
G. Use the H_2 routing surface (D) to place spur lines that connect BECCS-H_2, ATR-H_2, and H_2-using facilities to the trunk line along the shortest route and while following existing natural gas pipeline corridors as much as possible. Arbitrarily limit maximum spur line length to 120 km.
H. Add ArcGIS Pro [36] supplied topographic base map (credits are shown on each map).

References

1. A. Pascale and E.D. Larson, "Iron and Steel Industry Transition," draft Annex J to *Net-Zero America: Potential pathways, infrastructure, and impacts*, 23 November 2020.
2. Roadmap to US Hydrogen Economy *FCHEA*, p. 20 (2021)
3. Energy Information Administration, Natural Gas Consumption by End Use, website accessed March 2021.
4. Naturalgas.org, The Transportation of Natural Gas, accessed March 2021.
5. U.S. DRIVE, *Hydrogen Delivery Technical Team Roadmap*, United States Driving Research and Innovation for Vehicle efficiency and Energy sustainability, July 2017.
6. Energy Transitions Commission, *Making the Hydrogen Economy Possible: Accelerating Clean Hydrogen in an Electrified Economy*," Version 1.2, The Making Mission Possible Series, April 2021.
7. Northern Gas Networks, Equinor, and Cadent, *H21 North of England*, H21 NoE Report/2018, 2018.
8. E. Baik and E.D. Larson, "Bioenergy Supply Transition Analysis," draft Annex H to *Net-Zero America: Potential pathways, infrastructure, and impacts*, 18 November 2020.
9. E. Leslie, A. Pascale, and J.D. Jenkins, "Solar and Wind Generation Transitions," draft Annex D to *Net-Zero America: Potential pathways, infrastructure, and impacts*, 5 January 2021.
10. C. Greig and A. Pascale, "CO2 transport and storage infrastructure transition analysis," draft Annex I to *Net-Zero America: Potential pathways, infrastructure, and impacts*, 5 January 2021.
11. Pacific Northwest National Laboratory, Hydrogen Analysis Resource Center, spreadsheet Hydrogen Pipelines 2016.xlsx, accessed online 29 March 2021.
12. The Hydrogen Council, *Path to hydrogen competitiveness: a cost perspective*, Jan. 20, 2020. (PDF accessed online 29 March 2021.)
13. Air Products, *Air Products U.S. Gulf Coast hydrogen network*, 2012. (PDF accessed online 29 March 2021.)
14. Air Liquide, *Mississippi River Pipeline and Utility Services*, 2015. (PDF accessed online 29 March 2021.)
15. Pipeline Association of Louisiana, *Pipeline Safety Training For First Responders*, 2020. (PDF accessed online 29 March 2021.)
16. Air Products, *Air Products Gulf Coast Connection Project*, 2012. (PDF accessed online 29 March 2021.)
17. Environmental Protection Agency, *Facility Level Information on Greenhouse Gases Tool (FLIGHT) database*, (2017 data accessed).
18. The Hydrogen Council, *A Perspective on Hydrogen Investment, Development, and Cost Competitiveness*, 2021. (PDF accessed online 29 March 2021.)
19. Bloomberg New Energy Finance, *Hydrogen Economy Outlook*, March 30, 2020.
20. International Renewable Energy Agency, Renewable Power Generation Costs, 2019.
21. M. Ziegler and J. Tancik, "Re-examining rates of lithium-ion battery technology improvement and cost decline," *Energy and Environmental Science*, March 23, 2021.
22. G. del Álamo, J. Sandquist, B.J. Vreugdenhil, G. Aranda Almansa, and M. Carbo, *Implementation of bio-CCS in biofuels production*, IEA Bioenergy Task 33 special report, 2018.
23. J. C. Meerman and E. D. Larson, "Negative-carbon drop-in transport fuels produced: Via catalytic hydropyrolysis of woody biomass with CO2 capture and storage," *Sustain. Energy Fuels*, vol. 1, no. 4, pp. 866–881, 2017, doi:10.1039/c7se00013h.
24. C. Greig, E. Larson, T. Kreutz, J. Meerman, and R. Williams, *Lignite-plus-Biomass to Synthetic Jet Fuel with CO2 Capture and Storage: Design, Cost, and Greenhouse Gas Emissions Analysis for a Near-Term First-of-a-Kind Demonstration Project and Prospective Future Commercial Plants*, Final report to National Energy Technology Laboratory under contract FE0023697, 2017. https://www.osti.gov/biblio/1438250.

25. P. Capros, E. Dimopoulou, S. Evangelopoulou, T. Fotiou, M. Kannavou, P. Siskos, G. Zazias L. de Vos, A. Dadkhah, and G. Dekelver, *Technology pathways in decarbonisation scenarios*, Advanced System Studies for Energy Transition Project, July 2018.

26. J. Davison (project manager), CO2 Capture at Coal Based Power and Hydrogen Plants," Report 2014/03, IEAGHG, May 2014, 1028 pages.

27. ENEA Consulting, "The Potential of Power-To-Gas," January 2016.

28. B.D. James, D.A. DeSantis, and G. Saur, *Final Report: Hydrogen Production Pathways Cost Analysis (2013 – 2016)*, DOE-StrategicAnalysis-6231-1, 30 September 2016.

29. T. G. Kreutz, E. D. Larson, C. Elsido, E. Martelli, C. Greig, and R. H. Williams, Techno-economic prospects for producing Fischer-Tropsch jet fuel and electricity from lignite and woody biomass with CO_2 capture for EOR, *Appl. Energy*, vol. 279, no. August, p. 115841, 2020.

30. T. Fout, A. Zoelle, D. Keairns, M. Turner, M. Woods, N. Kuehn, V. Shah, V. Chou, and L. Pinkerton, *Cost and Performance Baseline for Fossil Energy Plants Volume 1b: Bituminous Coal (IGCC) to Electricity Revision 2b – Year Dollar Update*, DOE/NETL-2015/1727, National Energy Technology Laboratory, 31 July 2015.

31. J. Laumb, Advanced coal-fired power cycles, 54th Annual Minnesota Power Systems Conference, St. Paul, MN, 6-8 Nov 2018.

32. R. Jones (Co-Founder, Evolved Energy Research), personal communication, 2020.

33. E. S. M. D. Classification Development Branch, "North American Industry Classification System (NAICS) Main Page," Mar. 05, 2019. https://www.census.gov/eos/www/naics/ (accessed Mar. 06, 2019).

34. Energy Information Administration, "Assumptions to Annual Energy Outlook - Industrial Demand Module." Jul. 2018. https://www.eia.gov/outlooks/aeo/assumptions/pdf/industrial.pdf (accessed Jan. 24, 2019).

35. HIFLD, "Natural Gas Pipelines," *Homeland Infrastructure Foundation-Level Data (HIFLD)*, Aug. 24, 2019. https://hifld-geoplatform.opendata.arcgis.com/datasets/natural-gas-pipelines (accessed June 9, 2020).

36. Environmental Systems Research Institute (ESRI), *ArcGIS Pro*. 2020. https://arcgis.pro/.